Single-Shot All-Optical Switching in CoFeB/MgO Magnetic Tunnel Junctions

Junta Igarashi,[1,2] Sébastien Geiskopf,[1] Takanobu Shinoda,[3,4] Butsurin Jinnai,[5] Yann Le Guen,[1] Julius Hohlfeld,[1] Shunsuke Fukami,[3,4,5,6,7,1,8] Hideo Ohno,[3,4,5,6,7] Jon Gorchon,[1] Stéphane Mangin,[1,6] Michel Hehn,[1,6] and Grégory Malinowski[1]

[1)] *Université de Lorraine, CNRS, IJL, Nancy, France*

[2)] *Global Research and Development Center for Business by Quantum-AI technology (G-QuAT), National Institute of Advanced Industrial Science and Technology, Tsukuba, Japan*

[3)] *Laboratory for Nanoelectronics and Spintronics, Research Institute of Electrical Communication, Tohoku University, Sendai, Japan*

[4)] *Department of Electronic Engineering, Tohoku University, Sendai, Japan*

[5)] *Advanced Institute for Materials Research, Tohoku University, Sendai, Japan*

[6)] *Center for Science and Innovation in Spintronics, Tohoku University, Sendai, Japan.*

[7)] *Center for Innovative Integrated Electronic Systems, Tohoku University, Sendai, Japan.*

[8)] *Inamori Research Institute for Science, Kyoto, Japan.*

(*Electronic mail: junta.igarashi@aist.go.jp)

(Dated: 30 October 2025)

We demonstrate single-shot all-optical switching (AOS) in rare-earth-free CoFeB/MgO magnetic tunnel junctions (MTJs), a material system widely adopted in spin-transfer torque magnetic random-access memory (STT-MRAM). By tuning the capping layer thickness, we show that precise heat control enables deterministic magnetization reversal from parallel (P) to antiparallel (AP) state. Furthermore, we detect magnetization reversal in a micro-scale MTJ device via the tunnel magnetoresistance (TMR) effect. Our findings suggest that ultrafast spin transport or dipolar interactions—or a combination of both—may play essential roles in the switching process. This work represents a significant step toward integrating AOS with MTJ technology.

I. INTRODUCTION

The ultrafast manipulation of magnetization has attracted considerable attention for both fundamental research and technological applications. The field of ultrafast magnetism was initiated by the discovery of ultrafast demagnetization—an abrupt reduction in magnetization within a picosecond—induced by femtosecond laser excitation[1]. Subsequently, in Co/Pt multilayer-based spin valves with symmetric ferromagnetic layers, it was observed that the demagnetization time depends on the initial magnetic configuration, either parallel (P) or antiparallel (AP) state[2]. This behavior has been attributed to nonlocal spin transport between the two ferromagnetic layers, triggered by ultrafast demagnetization in each layer[3,4]. In particular, in the AP state, demagnetization is accelerated by spin currents carrying opposite spin polarization injected from the adjacent ferromagnetic layer. While such ultrafast spin currents can effectively manipulate magnetization dynamics, at that stage they did not lead to full magnetization reversal.

For many years, it was widely believed that single-shot all-optical switching (AOS) could not be achieved in purely ferromagnetic systems, in contrast to certain ferrimagnets such as Gd-based alloys, multilayers, and MnRuGa[5–10]. In this context, Igarashi *et al.* reported in 2023 that single-shot AOS can be realized in a Co/Pt-based spin valve by introducing structural asymmetry between the two ferromagnetic layers, such as differences in Co layer thickness and the number of Co/Pt repetitions[11]. Depending on the laser fluence, two types of magnetization switching were observed: AP-to-P switching at high fluence and P-to-AP switching at low fluence. The former can be explained by nonlocal spin transport, as discussed above. The latter, however, is counterintuitive. Based on time-resolved experiments reported in a previous study[11], nonlocal spin transport is also believed to contribute to P-to-AP switching. To date, two possible scenarios have been proposed: (i) spin currents generated during the remagnetization of the reference layer, and (ii) spin currents produced by the demagnetization of the free layer, followed by spin-flip reflection at the interface between the Cu spacer and the reference layer[12]. Recently, detailed time-resolved experiments revealed that P-to-AP switching occurs on the timescale of the reference layer's remagnetization, supporting the first scenario[13]. Furthermore, it has been demonstrated that single-shot AOS can occur even without direct laser excitation, suggesting that complete demagnetization of the free layer in the spin valve—triggered by a rapid rise in electronic temperature due to ultrafast stimuli such as optical or thermal pulses—is a key requirement for AOS in such systems[14].

In recent years, increasing attention has been paid to integrating magnetic tunnel junctions (MTJs)—the core components of spin-transfer torque magnetic random-access memory (STT-MRAM)—with AOS technology[15–20]. In the earliest report, GdFeCo, a well-established all-optically switchable material, was used as the free layer in an MTJ structure. Although single-shot AOS could be detected via the tunnel magnetoresistance (TMR) effect[21], the observed TMR ratio was relatively low, around 0.6%[15]. Later studies introduced composite free layers composed of CoFeB exchange-coupled with all-optically switchable materials such as Co/Tb multilayers[17,19,20], Gd/Co bilayers[18], and GdCo alloys with in-plane magnetic anisotropy[22] to improve the TMR ratio. However, the use of rare-earth elements remains impractical for device integration due to their poor thermal stability, particularly under the annealing conditions required for MTJ fabrication.

Inspired by previous studies showing that demagnetization dynamics in symmetric MTJ structures depend on the initial magnetic configuration[23], similar to ferromagnetic spin valves[2], we explore the possibility of single-shot AOS in MTJs with asymmetric structures. These findings suggest that structural asymmetry could enable single-shot AOS, as demonstrated in spin valves[11]. By optimizing the MTJ capping layer thickness, we achieve single-shot AOS in CoFeB/MgO-based MTJs without the use of rare-earth elements, and detect the switching via the TMR effect in microscale devices.

II. EXPERIMENTAL METHOD

In this section, we describe the MTJ stack, its characterization, and the experimental procedure for the single-shot AOS measurements.

A. MTJ stack

We employ a standard de facto MTJ structure, consisting of a CoFeB free layer with a perpendicular easy axis to the sample plane[24], and a synthetic ferrimagnetic (SyF) reference layer[25], as illustrated in Fig. 1(a). All samples were fabricated by sputtering. The basic layer stack is as follows (thicknesses in nanometers): Ta(5)/Pt(5)/[Co(0.4)/Pt(0.6)]$_6$/Co(0.4)/Ru(0.4)/[Co(0.4)/Pt(0.4)]$_2$/Co(0.4)/Ta(0.2)/CoFeB(1)/MgO(t_{MgO})/CoFeB(1.5)/Ta(5)/Capping(t_{cap}), deposited on a sapphire or thermally oxidized Si substrate. The sample deposited on a sapphire substrate was used for AOS measurements, while the one deposited on a thermally oxidized Si substrate was used for sample characterization, as described in the next section. After deposition, the MTJ stack was annealed at 300°C for 1 hour. We define the layers separated by the MgO barrier as the SyF reference layer (bottom, closer to the substrate) and the CoFeB free layer (top, farther from the substrate), as shown in Fig. 1(a). Thickness of the MgO layer t_{MgO} are 1.3 and 2.0 nm. For the capping layer, we use either Ru or Pt. The capping layer thicknesses t_{cap} used in this study are 0, 1.0, 2.0, 3.0, 4.0, and 5.0 nm for Ru, and 2.5 and 5.0 nm for Pt.

B. Sample characterization

Prior to the experiments, we characterize the MTJ stacks. Due to experimental constraints, the MTJ stacks were deposited on thermally oxidized Si wafers. It should be noted that the stack properties are expected to be nearly identical regardless of the substrate used. Figure 1(b) shows the magnetization curves measured using a vibrating sample magnetometer (VSM). A perpendicular easy axis is confirmed in both the

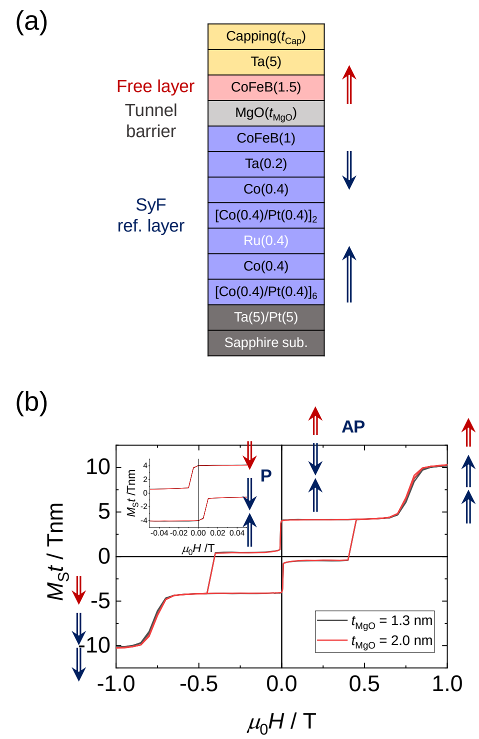

FIG. 1. MTJ stack and its characterization. (a) Schematic of the MTJ stack structure used in this study. (b) *M–H* curves measured for MTJ stacks with $t_{\mathrm{MgO}} = 1.3$ and 2.0 nm. The inset shows a magnified view. Arrows indicate the corresponding magnetic configurations.

free and reference layers. The corresponding magnetic configurations are illustrated in Fig. 1(b). In this study, we focus on the P and AP states, as indicated in the figure.

Next, we evaluate the resistance-area product (RA) and the tunnel magnetoresistance (TMR) ratio using the current-in-plane tunneling (CIPT) method, which enables characterization of these parameters without device fabrication[26]. Due to probe limitations, the measurement was performed only for the MTJ stack with $t_{\mathrm{MgO}} = 1.3$ nm. The measured TMR ratio and RA value are 158% and 30 $\Omega\,\mu\mathrm{m}^2$, respectively.

C. Single-shot switching experiment

The experimental setup used in this study is identical to that described in Ref.[11]. Linearly polarized laser pulses were generated using a Ti:sapphire femtosecond laser system with a central wavelength of 800 nm and a repetition rate of 5 kHz. The pulse duration was varied from 50 fs to 10 ps. The $1/e$ spot size $2\omega_0$ is approximately 80 μm.

To visualize the magnetic domain states, magneto-optical Kerr effect (MOKE) imaging was performed using a light-emitting diode (LED) with a center wavelength of 628 nm[27]. The pump beam was incident on the sample at an angle of 45°[11]. A permanent magnet was used to apply an external magnetic field and to saturate the MTJ stack prior to laser pulse excitation. A schematic of the experimental setup is shown in Fig. 2.

III. EXPERIMENTAL RESULTS

In this section, we show experimental results obtained with MTJ stacks.

A. Single-shot AOS experiment

Figure 2(a) shows MOKE images obtained after laser pulse irradiation with a pulse duration of 50 fs for samples with a Ru capping layer thickness (t_{Ru}) of 5.0 nm and $t_{MgO} = 1.3$ nm, initially in both the P (blue) and AP (red) states. While no AP-to-P switching is observed, clear P-to-AP switching is observed. We confirm that P-to-AP switching also occurs in a sample with $t_{MgO} = 2.0$ nm as shown in Fig. 2(b).

For quantitative comparison, we extract the threshold fluences for P-to-AP switching (F_P) and multidomain formation (F_{MD}) by fitting the domain area as a function of laser pulse energy, as described in the Supplementary Material of Ref.[28]. Figures 3(a) and (b) summarize the threshold fluences as a function of t_{cap} for $t_{MgO} = 1.3$ and 2.0 nm, respectively. As shown in figures, the trends are essentially independent of MgO thickness. For P-to-AP switching, F_P remains nearly constant with varying capping layer thickness, whereas F_{MD} increases with t_{cap}. Unlike previous studies on Co/Pt-based spin valves[11,28], AP-to-P switching is not observed in these MTJ stacks.

Since the only structural difference between the samples is the Ru capping thickness, we infer that laser-induced heating of the ferromagnetic layers in MTJ stacks plays a key role, similar to findings reported in Ref.[14]. To test this hypothesis, we performed the same experiment using Pt capping, which has comparable refractive indices to Ru. The results obtained with Pt capping are shown as open symbols in Fig.3 (a). As expected, F_P with Pt capping is nearly identical to that with Ru capping. The F_{MD} values with Pt capping also follow the same trend as those with Ru.

Furthermore, we calculate the laser energy absorption in the free and reference layers using the transfer matrix method, as shown in Fig. 3(c). The refractive indices of each material were obtained from Refs.[29,30]. As shown in Fig. 3(c), increasing the thickness of the capping layer leads to a reduction in laser energy absorption in the reference layer. Although the energy absorption in the free layer also decreases with increasing capping thickness, the change is relatively small compared to that in the reference layer. This is because thicker Ru or Pt capping layers absorb more of the incident laser energy. Consequently, the total energy absorption in the capping plus free layers increases monotonically with capping layer thickness, as indicated in the figure. These experimental and simulation results suggest that enhancing the heating of the free layer (including the capping layer) while suppressing laser-induced heating of the reference layer facilitates the observation of P-to-AP switching. This finding is consistent with conclusions drawn from previous studies using spin-valve structures[11,14].

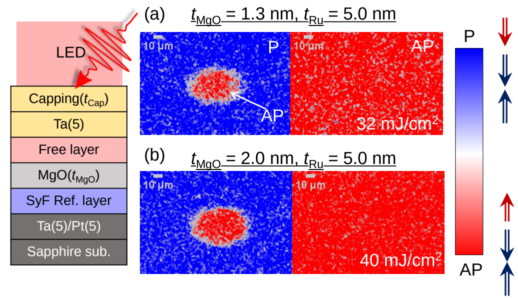

FIG. 2. Single-shot magnetization switching observed via MOKE imaging in MTJ stacks with a Ru capping layer thickness of $t_{Ru} = 5.0$ nm. (a) $t_{MgO} = 1.3$ nm, (b) $t_{MgO} = 2.0$ nm. For both cases, MOKE images are shown after laser irradiation, starting from the P (blue) and AP (red) states.

In addition to laser-induced heating, ultrafast hot electron pulses generated by laser excitation of a nonmagnetic layer have been shown to efficiently transport energy and induce ultrafast demagnetization[31–33], and even magnetization reversal[14,34,35]. This effect may also contribute to efficient heating of the free layer.

We also investigate pulse duration dependence of the P-to-AP switching. See Appendix for more details.

B. Single-shot AOS detected via TMR effect

Having observed P-to-AP switching in MTJ stacks, our next objective is to detect P-to-AP switching via the tunnel magnetoresistance (TMR) effect in an MTJ device. To this end, we fabricated microscale MTJ devices with an MgO thickness of $t_{MgO} = 2.0$ nm and $t_{Ru} = 3.0$ nm. The fabrication process followed the procedure described in Ref.[22]. In this study, the ion milling was stopped at the Pt buffer layer to prevent domain nucleation in the reference layer caused by laser irradiation. An optical micrograph of the fabricated MTJ device is shown in Fig. 4(a). The device has lateral dimensions of $10 \times 10 \mu m^2$. Due to technical constraints, the use of transparent electrodes was not feasible. Therefore, to enable optical access while simultaneously measuring the MTJ resistance, a Ti/Au electrode was designed to cover approximately 30 % of the MTJ pillar, as in the previous study[22], as illustrated in Figs. 4(a) and (b).

We employ the same experimental setup as described in the previous study[22], in which a laser pulse is applied to the MTJ device while simultaneously measuring its resistance. The $1/e$ spot size $2\omega_0$ is approximately 110 μm. A voltage of 30 mV is applied using a source meter (Keithley 2400) to monitor the MTJ resistance. Prior to laser irradiation, the MTJ device is initialized to either the P or AP state using a permanent magnet.

Figure 4(c) shows the measured resistance of the MTJ device. The black symbols in Figs.4(c) and (d) represent magnetization reversal induced by an external magnetic field. After device fabrication, the TMR ratio is reduced from 158 %

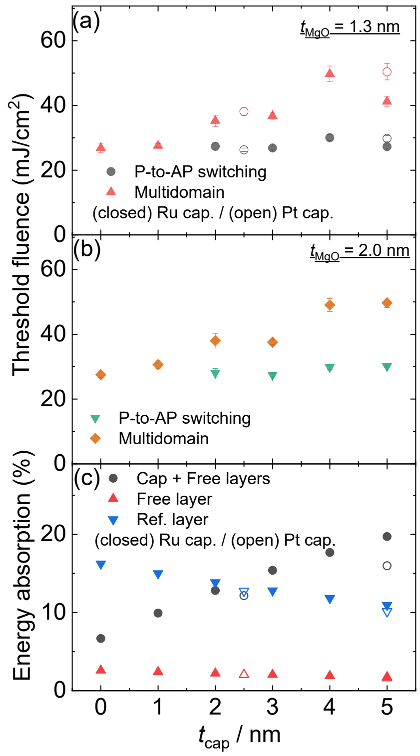

FIG. 3. Summary of single-shot switching experiments in MTJ stacks. (a, b) Evolution of the threshold fluences for P-to-AP switching (F_P) and multidomain formation (F_{MD}) as a function of capping layer thickness t_{cap} for (a) $t_{MgO} = 1.3$ nm and (b) $t_{MgO} = 2.0$ nm. (c) Calculated laser energy absorption in the capping, free, and reference layers as a function of t_{cap}. Closed (open) symbols represent MTJ stacks with Ru (Pt) capping layers.

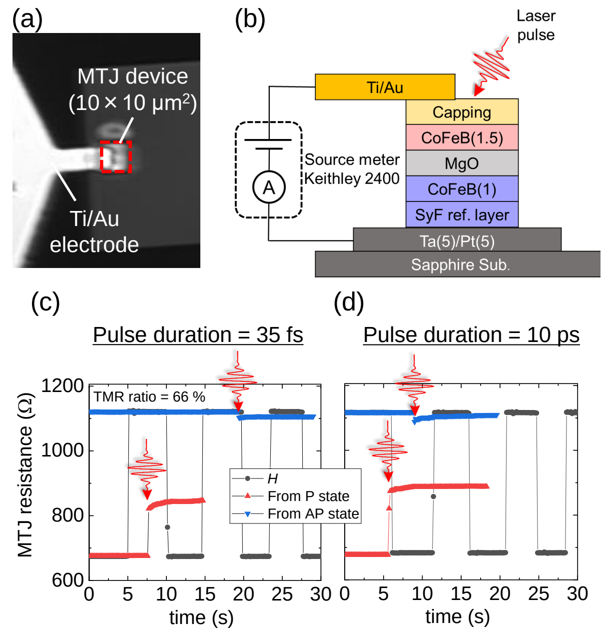

FIG. 4. Single-shot switching detected via the TMR effect. (a) Optical microscopy image of the MTJ device. (b) Schematic of the experimental setup. (c, d) (c,d) Time dependence of MTJ resistance in response to a square-wave magnetic field (black lines) and to irradiation of the P (red line) and AP state (blue line) by single laser pulses with the timing indicated by the laser pulse arrows. The pulse durations and fluences were (c) 35 fs and 21.6 mJ/cm^2, and (d) 10 ps and 41.0 mJ/cm^2, respectively.

to 66 %, likely due to processing damage during microfabrication. However, it is worth mentioning that the MTJ stack employed here is already used in STT-MRAM production, indicating that this issue can potentially be solved by adopting optimized fabrication processes. In addition, MTJ devices utilizing transparent electrodes have been fabricated while maintaining high TMR ratio[36,37]. In Fig. 4(c), a clear change in the MTJ resistance is observed only when the initial magnetic state is the P state (red trace), indicating a P-to-AP switching occurs. Due to the partial coverage of the device by the Ti/Au electrode, full P-to-AP switching across the entire junction area was not observed, consistent with a previous finding[22]. To further investigate the pulse-duration dependence, we also perform the same measurement using 10 ps laser pulse. As demonstrated in the full-film experiments in Appendix A (Fig. 5), P-to-AP switching could again be detected via the TMR effect, confirming the robustness of this phenomenon in patterned devices as well. The dependence of the switching behavior on laser fluence is summarized in Appendix B.

IV. DISCUSSION

We have demonstrated single-shot P-to-AP switching in CoFeB/MgO-based MTJ stacks and devices, which adopt the same structure as those used in STT-MRAM technology. In this section, we discuss possible mechanisms underlying the observed P-to-AP switching.

While we initially expected that the P-to-AP switching in MTJ stacks would result from ultrafast spin transport—as previously reported in ferromagnetic spin valves[11]—the precise mechanism remains elusive. In addition to ultrafast spin transport, coupling between the free and reference layers may also contribute to the switching process, similar to the mechanism in heat-assisted magnetic recording (HAMR)[38].

To explore this possibility, we measured the magnetic hysteresis loop using the magneto-optical Kerr effect (MOKE), as presented in Appendix C. Figure 7 shows a small shift field that biases the MTJ toward the AP state. Although the synthetic antiferromagnetic (SyF) reference layer is designed to suppress such a shift field, it might affect the final magnetic state.

Time-resolved MOKE (TR-MOKE) experiments could provide further insights by distinguishing between the two possible mechanisms—ultrafast spin-current-induced switching and thermally assisted field-driven switching—due to their differing timescales[28]. However, the complex multilayer structure of the MTJ stacks used in this study makes TR-MOKE measurements technically challenging. If similar P-to-AP switching can be achieved in a simplified MTJ stack, for example, one without a SyF reference layer, it may be possible to directly measure the magnetization reversal dynamics using TR-MOKE techniques.

Although the detailed mechanism of the switching remains to be clarified, our results demonstrate that single-shot magnetization reversal can be induced by carefully controlling the energy absorption ratio between the free and reference layers. In this proof-of-concept study, we employed a free layer consisting of a single CoFeB layer. However, the proposed approach is applicable to more practical structures, such as [CoFeB/MgO] multilayers, which are better suited for memory applications[39–41].

V. CONCLUSION

We have demonstrated single-shot AOS in CoFeB/MgO-based MTJs without relying on rare-earth elements, using a structure compatible with STT-MRAM technology. Although complete switching of the entire MTJ area was not achieved due to the shadowing effect of the electrode[22], we have shown that this single-shot AOS can be electrically detected via the TMR effect in a microscale MTJ device.

Our combined experimental and numerical results highlight the importance of precise thermal management for enabling deterministic magnetization reversal in this system. While the underlying physical mechanisms remain to be fully understood, this study establishes a crucial link between ultrafast magnetism and spintronic device platforms. Our findings represent an important step toward the integration of AOS into practical MTJ-based memory technologies.

ACKNOWLEDGMENTS

We thank E. Díaz, A. Anadón, J.-X. Lin, L. D. Buda-Prejbeanu, R. C. Sousa, I. L. Prejbeanu, K. Ishibashi, S. Iihama, J.-Y. Yoon, T. Arakawa, N.-H. Kaneko for fruitful discussion. This work is supported by the French National Research Agency (ANR) through the France 2030 government PEPR Electronic grants EMCOM (ANR-22-PEEL-0009) by the ANR SPOTZ project ANR- 20-CE24-0003, SLAM ANR- 23-CE30-0047, the project MAT-PULSE from "Lorraine Université d'Excellence" reference ANR-15-IDEX-04-LUE, the Institute Carnot ICEEl, the Région Grand Est, the Metropole Grand Nancy, the "FEDERFSE Lorraine et Massif Vosges 2014-2020", a European Union Program, the Academy of Finland (Grant No. 316857), the Sakura Program, the JSPS Bilateral Program, JSPS KAKENHI JP 24K22964, 24H02235, 24H00039, MEXT Initiative to Establish Next-generation Novel Integrated Circuits Centers (X-NICS) (Grant No. JPJ011438), the Tohoku University-Université de Lorraine Matching Funds, and CSIS cooperative research project in Tohoku University. The devices in the present study were patterned at MiNaLor platform which is partially funded by Grand Est Region and Feder through RaNGE project. The devices in the present study were patterned at MiNaLor platform which is partially funded by Grand Est Region and Feder through RaNGE project. This article is based upon work from COST Action CA23136 CHIROMAG, supported by COST (European Cooperation in Science and Technology). J.I. acknowledges support from JSPS Overseas Research Fellowships. All funding was shared equally among all authors.

DATA AVAILABILITY STATEMENT

The data that support the findings of this study are available from the corresponding author upon reasonable request.

REFERENCES

[1] E. Beaurepaire, J.-C. Merle, A. Daunois, and J.-Y. Bigot, "Ultrafast spin dynamics in ferromagnetic nickel," Physical review letters **76**, 4250 (1996).

[2] G. Malinowski, F. Dalla Longa, J. Rietjens, P. Paluskar, R. Huijink, H. Swagten, and B. Koopmans, "Control of speed and efficiency of ultrafast demagnetization by direct transfer of spin angular momentum," Nature Physics **4**, 855–858 (2008).

[3] A. Schellekens, K. Kuiper, R. De Wit, and B. Koopmans, "Ultrafast spin-transfer torque driven by femtosecond pulsed-laser excitation," Nature communications **5**, 4333 (2014).

[4] G.-M. Choi, B.-C. Min, K.-J. Lee, and D. G. Cahill, "Spin current generated by thermally driven ultrafast demagnetization," Nature communications **5**, 4334 (2014).

[5] I. Radu, K. Vahaplar, C. Stamm, T. Kachel, N. Pontius, H. Dürr, T. Ostler, J. Barker, R. Evans, R. Chantrell, *et al.*, "Transient ferromagnetic-like state mediating ultrafast reversal of antiferromagnetically coupled spins," Nature **472**, 205–208 (2011).

[6] T. Ostler, J. Barker, R. Evans, R. Chantrell, U. Atxitia, O. Chubykalo-Fesenko, S. El Moussaoui, L. Le Guyader, E. Mengotti, L. Heyderman, *et al.*, "Ultrafast heating as a sufficient stimulus for magnetization reversal in a ferrimagnet," Nat. Commun. **3**, 666 (2012).

[7] M. Lalieu, M. Peeters, S. Haenen, R. Lavrijsen, and B. Koopmans, "Deterministic all-optical switching of synthetic ferrimagnets using single femtosecond laser pulses," Phys. Rev. B **96**, 220411 (2017).

[8] C. Banerjee, N. Teichert, K. Siewierska, Z. Gercsi, G. Atcheson, P. Stamenov, K. Rode, J. Coey, and J. Besbas, "Single pulse all-optical toggle switching of magnetization without gadolinium in the ferrimagnet Mn2RuxGa," Nat. Commun. **11**, 4444 (2020).

[9] C. Davies, G. Bonfiglio, K. Rode, J. Besbas, C. Banerjee, P. Stamenov, J. Coey, A. Kimel, and A. Kirilyuk, "Exchange-driven all-optical magnetic switching in compensated 3 d ferrimagnets," Phys. Rev. Res. **2**, 032044 (2020).

[10] C. Banerjee, K. Rode, G. Atcheson, S. Lenne, P. Stamenov, J. Coey, and J. Besbas, "Ultrafast double pulse all-optical reswitching of a ferrimagnet," Phys. Rev. Lett. **126**, 177202 (2021).

[11] J. Igarashi, W. Zhang, Q. Remy, E. Díaz, J.-X. Lin, J. Hohlfeld, M. Hehn, S. Mangin, J. Gorchon, and G. Malinowski, "Optically induced ultrafast magnetization switching in ferromagnetic spin valves," Nature Materials **22**, 725–730 (2023).

[12] Q. Remy, "Ultrafast magnetization reversal in ferromagnetic spin valves: An s- d model perspective," Physical Review B **107**, 174431 (2023).

[13] H. Singh, A. Anadón, J. Igarashi, Q. Remy, S. Mangin, M. Hehn, J. Gorchon, and G. Malinowski, "Ultrafast spin accumulations drive magnetization reversal in multilayers," arXiv preprint arXiv:2508.19675 (2025).

[14] K. Ishibashi, J. Igarashi, A. Anadón, M. Hehn, Y. Le Guen, S. Iihama, J. Hohlfeld, J. Gorchon, S. Mangin, and G. Malinowski, "Single-shot magnetization reversal in ferromagnetic spin valves via heat control," Physical Review Letters **135**, 116702 (2025).

[15]J.-Y. Chen, L. He, J.-P. Wang, and M. Li, "All-optical switching of magnetic tunnel junctions with single subpicosecond laser pulses," Physical Review Applied **7**, 021001 (2017).
[16]A. V. Kimel and M. Li, "Writing magnetic memory with ultrashort light pulses," Nature Reviews Materials **4**, 189–200 (2019).
[17]L. Avilés-Félix, A. Olivier, G. Li, C. S. Davies, L. Álvaro-Gómez, M. Rubio-Roy, S. Auffret, A. Kirilyuk, A. Kimel, T. Rasing, *et al.*, "Single-shot all-optical switching of magnetization in tb/co multilayer-based electrodes," Scientific reports **10**, 5211 (2020).
[18]L. Wang, H. Cheng, P. Li, Y. L. Van Hees, Y. Liu, K. Cao, R. Lavrijsen, X. Lin, B. Koopmans, and W. Zhao, "Picosecond optospintronic tunnel junctions," Proceedings of the National Academy of Sciences **119**, e2204732119 (2022).
[19]S. Mondal, D. Polley, A. Pattabi, J. Chatterjee, D. Salomoni, L. Aviles-Felix, A. Olivier, M. Rubio-Roy, B. Diény, L. D. B. Prejbeanu, *et al.*, "Single-shot switching in tb/co-multilayer based nanoscale magnetic tunnel junctions," Journal of Magnetism and Magnetic Materials **581**, 170960 (2023).
[20]D. Salomoni, Y. Peng, L. Farcis, S. Auffret, M. Hehn, G. Malinowski, S. Mangin, B. Dieny, L. Buda-Prejbeanu, R. C. Sousa, *et al.*, "Field-free all-optical switching and electrical readout of tb/co-based magnetic tunnel junctions," Physical Review Applied **20**, 034070 (2023).
[21]M. Julliere, "Tunneling between ferromagnetic films," Physics letters A **54**, 225–226 (1975).
[22]S. Geiskopf, J. Igarashi, G. Malinowski, J.-X. Lin, J. Gorchon, S. Mangin, J. Hohlfeld, D. Lacour, and M. Hehn, "Single-shot all-optical magnetization switching in in-plane magnetized magnetic tunnel junction," Applied Physics Letters **126** (2025).
[23]W. He, T. Zhu, X.-Q. Zhang, H.-T. Yang, and Z.-H. Cheng, "Ultrafast demagnetization enhancement in cofeb/mgo/cofeb magnetic tunneling junction driven by spin tunneling current," Scientific Reports **3**, 2883 (2013).
[24]S. Ikeda, K. Miura, H. Yamamoto, K. Mizunuma, H. Gan, M. Endo, S. Kanai, J. Hayakawa, F. Matsukura, and H. Ohno, "A perpendicular-anisotropy cofeb–mgo magnetic tunnel junction," Nature materials **9**, 721–724 (2010).
[25]H. Sato, M. Yamanouchi, S. Ikeda, S. Fukami, F. Matsukura, and H. Ohno, "Mgo/cofeb/ta/cofeb/mgo recording structure in magnetic tunnel junctions with perpendicular easy axis," IEEE Transactions on Magnetics **49**, 4437–4440 (2013).
[26]D. Worledge and P. Trouilloud, "Magnetoresistance measurement of unpatterned magnetic tunnel junction wafers by current-in-plane tunneling," Applied Physics Letters **83**, 84–86 (2003).
[27]S. Iihama, Y. Xu, M. Deb, G. Malinowski, M. Hehn, J. Gorchon, E. E. Fullerton, and S. Mangin, "Single-Shot Multi-Level All-Optical Magnetization Switching Mediated by Spin Transport," Adv. Mater. **30**, 1804004 (2018).
[28]J. Igarashi, Y. Le Guen, J. Hohlfeld, S. Mangin, J. Gorchon, M. Hehn, and G. Malinowski, "Influence of interlayer exchange coupling on ultrafast laser-induced magnetization reversal in ferromagnetic spin valves," Physical Review B **109**, 094422 (2024).
[29]P. Johnson and R. Christy, "Optical constants of transition metals: Ti, v, cr, mn, fe, co, ni, and pd," Phys. Rev. B **9**, 5056 (1974).
[30]J. Igarashi, Q. Remy, S. Iihama, G. Malinowski, M. Hehn, J. Gorchon, J. Hohlfeld, S. Fukami, H. Ohno, and S. Mangin, "Engineering single-shot all-optical switching of ferromagnetic materials," Nano Lett. **20**, 8654–8660 (2020).
[31]N. Bergeard, M. Hehn, S. Mangin, G. Lengaigne, F. Montaigne, M. Lalieu, B. Koopmans, and G. Malinowski, "Hot-electron-induced ultrafast demagnetization in co/pt multilayers," Physical review letters **117**, 147203 (2016).
[32]N. Bergeard, M. Hehn, K. Carva, P. Baláž, S. Mangin, and G. Malinowski, "Tailoring femtosecond hot-electron pulses for ultrafast spin manipulation," Applied Physics Letters **117** (2020).
[33]J.-E. Pudell, M. Mattern, M. Hehn, G. Malinowski, M. Herzog, and M. Bargheer, "Heat transport without heating?—an ultrafast x-ray perspective into a metal heterostructure," Advanced Functional Materials **30**, 2004555 (2020).
[34]R. Wilson, J. Gorchon, Y. Yang, C.-H. Lambert, S. Salahuddin, and J. Bokor, "Ultrafast magnetic switching of gdfeco with electronic heat currents," Physical Review B **95**, 180409 (2017).
[35]Y. Xu, M. Deb, G. Malinowski, M. Hehn, W. Zhao, and S. Mangin, "Ultrafast magnetization manipulation using single femtosecond light and hot-electron pulses," Advanced Materials **29**, 1703474 (2017).
[36]A. Olivier, L. Avilés-Félix, A. Chavent, L. Álvaro-Goémez, M. Rubio-Roy, S. Auffret, L. Vila, B. Dieny, R. C. Sousa, and I. Prejbeanu, "Indium tin oxide optical access for magnetic tunnel junctions in hybrid spintronic–photonic circuits," Nanotechnology **31**, 425302 (2020).
[37]T. Shibata, T. Mizuno, T. Nojiri, T. Yamane, Y. Hirata, W. Zhang, H. Fukuzawa, Y. Kasatani, and A. Tsukamoto, "Spin photo detector by using a cofeb magnetic tunnel junction," Journal of Physics D: Applied Physics **58**, 06LT01 (2024).
[38]M. H. Kryder, E. C. Gage, T. W. McDaniel, W. A. Challener, R. E. Rottmayer, G. Ju, Y.-T. Hsia, and M. F. Erden, "Heat assisted magnetic recording," Proceedings of the IEEE **96**, 1810–1835 (2008).
[39]H. Sato, M. Yamanouchi, S. Ikeda, S. Fukami, F. Matsukura, and H. Ohno, "Perpendicular-anisotropy cofeb-mgo magnetic tunnel junctions with a mgo/cofeb/ta/cofeb/mgo recording structure," Applied Physics Letters **101** (2012).
[40]K. Nishioka, H. Honjo, S. Ikeda, T. Watanabe, S. Miura, H. Inoue, T. Tanigawa, Y. Noguchi, M. Yasuhira, H. Sato, *et al.*, "Novel quad interface mtj technology and its first demonstration with high thermal stability and switching efficiency for stt-mram beyond 2xnm," in *2019 Symposium on VLSI Technology* (IEEE, 2019) pp. T120–T121.
[41]J. Igarashi, B. Jinnai, K. Watanabe, T. Shinoda, T. Funatsu, H. Sato, S. Fukami, and H. Ohno, "Single-nanometer cofeb/mgo magnetic tunnel junctions with high-retention and high-speed capabilities," npj Spintronics **2**, 1 (2024).

Appendix A: Pulse duration dependence

Here we present the pulse duration dependence of P-to-AP switching and multidomain formation. Figure 5 summarizes the evolution of the threshold fluences for both P-to-AP switching and multidomain states as a function of pulse duration for samples with $t_{\mathrm{Ru}} = 0$ nm and $t_{\mathrm{MgO}} = 1.3$ and 2.0 nm. As shown in Fig. 3, no P-to-AP switching is observed for a pulse duration of 50 fs. However, P-to-AP switching begins to emerge as the pulse duration increases for both structures. The threshold fluence for P-to-AP switching increases gradually with pulse duration, whereas that for multidomain formation shows a steeper increase. This contrast in their pulse-duration dependence is consistent with trends reported in previous studies[11,14]. The underlying mechanism for the observed P-to-AP switching at a pulse duration of 10 ps remains unclear. A previous study on ferromagnetic spin valves showed that the inclusion of a Cu heat sink extends the switching window up to 8 ps. In the present study, no such heat sink is applied to the MTJ stacks. One possible explanation is the use of sapphire substrates in this work, which offer superior heat dissipation compared to the glass substrates used in previous studies on ferromagnetic spin valves[11,14].

Appendix B: Fluence dependence

Here we present the results obtained under various laser fluences. Figure 6 shows the time evolution of MTJ resistance for different laser pulse fluences (pulse duration: 35 fs). When the initial state is parallel (P), the MTJ resistance begins to increase following laser irradiation at a fluence of 18.2 mJ/cm^2, indicating P-to-AP switching. In contrast, when

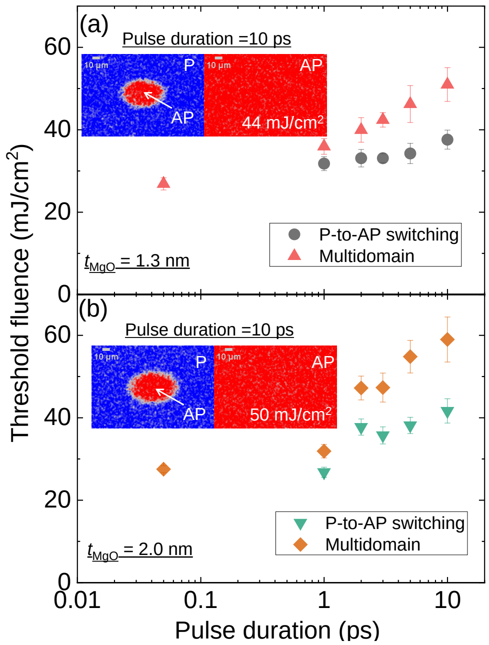

FIG. 5. (a, b) Evolution of the threshold fluences for P-to-AP switching (F_P) and multidomain formation (F_{MD}) as a function of pulse duration for (a) $t_{MgO} = 1.3$ nm and (b) $t_{MgO} = 2.0$ nm.

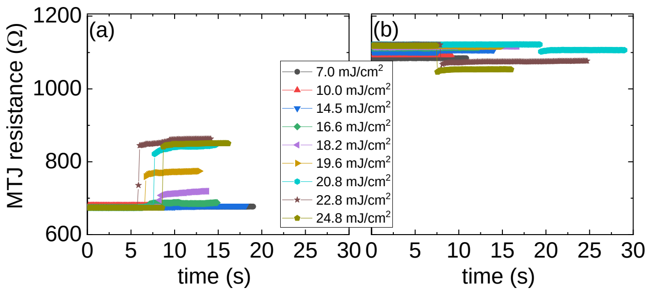

FIG. 6. Time evolution of MTJ resistance under various laser fluences with a pulse duration of 35 fs. (a) Initial magnetization in the parallel (P) state. (b) Initial magnetization in the antiparallel (AP) state.

starting from the AP state, no significant change in resistance is observed at comparable fluences. However, at fluences exceeding 19.6 mJ/cm^2, a slight decrease in resistance is observed even when the initial state is AP. This suggests the onset of multi-domain formation in the MTJ device at higher fluences.

Appendix C: MOKE Hysteresis Measurements

Here we present the results of MOKE hysteresis loop measurements performed on the MTJ stack. Figure 7 shows minor loops for two different magnetic configurations of the reference layer. In both cases, a small shift field is observed, which biases the magnetization toward the AP state. Although

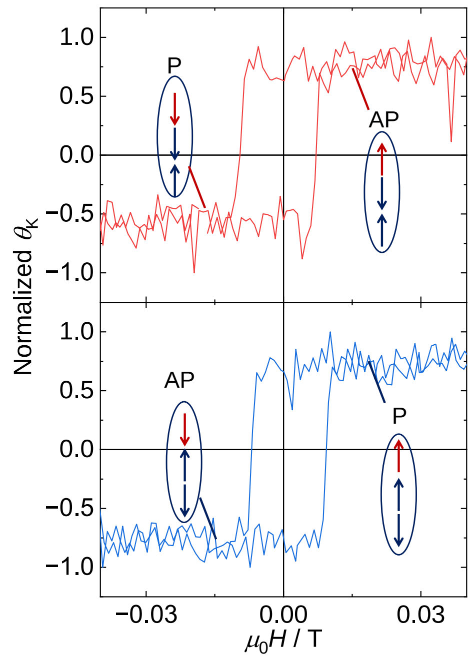

FIG. 7. Minor MOKE hysteresis loops of the MTJ stack. Arrows indicate the magnetic configuration corresponding to each MTJ state (P or AP). The wine-red and navy arrows represent the magnetization directions of the free and reference layers, respectively.

this shift field has only a minor influence under ambient conditions, it may become significant during laser pulse excitation, when the free layer is transiently demagnetized. Under such conditions, even a small bias field could be sufficient to drive the system into the AP state, in a manner analogous to HAMR[38]. However, it remains unclear how this shift field evolves after laser excitation.